

Using Undervolting as an On-Device Defense Against Adversarial Machine Learning Attacks

Saikat Majumdar, Mohammad Hossein Samavatian, Kristin Barber, Radu Teodorescu
Department of Computer Science and Engineering
The Ohio State University, Columbus, OH, USA
{majumdar.42, samavatian.1, barber.245, teodorescu.1}@osu.edu

Abstract—Deep neural network (DNN) classifiers are powerful tools that drive a broad spectrum of important applications, from image recognition to autonomous vehicles. Unfortunately, DNNs are known to be vulnerable to adversarial attacks that affect virtually all state-of-the-art models. These attacks make small imperceptible modifications to inputs that are sufficient to induce the DNNs to produce the wrong classification.

In this paper we propose a novel, lightweight adversarial correction and/or detection mechanism for image classifiers that relies on undervolting (running a chip at a voltage that is slightly below its safe margin). We propose using controlled undervolting of the chip running the inference process in order to introduce a limited number of compute errors. We show that these errors disrupt the adversarial input in a way that can be used either to correct the classification or detect the input as adversarial. We evaluate the proposed solution in an FPGA design and through software simulation. We evaluate 10 attacks on two popular DNNs and show an average detection rate of 80% to 95%.

Index Terms—undervolting, machine learning, defense

I. INTRODUCTION

Deep neural networks (DNNs) are emerging as the backbone of an increasing number of diverse applications. Some of these applications benefit from the deployment of sophisticated DNN models into so-called edge devices such as smartphones, smart home devices, autonomous driving systems, healthcare and many others [6], [33], [40]. Some of these applications, such as autonomous driving, are safety critical and their failure can endanger lives. Unfortunately, DNNs are known to be vulnerable to a variety of security threats. One of these threats is the so-called “adversarial attack” against DNN classifiers. The goal of these attacks is to induce the DNN to misclassify an input that the attacker controls, into the wrong class. For example, the image of a *STOP* sign can be slightly altered to cause a road sign recognition model to classify it as a *YIELD* sign in spite of it still looking like a *STOP* sign to the human eye. This is achieved by slightly altering the input to the classifier model in a way that induces it to produce erroneous an erroneous result.

A broad spectrum of prior work has demonstrated successful attacks on image classifiers and other computer vision applications [8], [10], [16], [28], [36], [41], [42], [47]. Prior work has also shown that virtually all classifiers are vulnerable including the popular ResNet [19], AlexNet [25], VGG [55]. The most recent, strongest attacks [8], [10] achieve reliable misclassification with changes to the input images that are small enough to be undetectable by casual observation.

In response to these attacks, prior work has proposed a suite a defenses [7], [12], [34], [35], [46], [62]. These defenses generally rely either on model retraining, which are not easily generalizable, or online, inference-time defenses, which are mostly software-based and have very high overheads. Only a few hardware-accelerated defenses have been proposed to date. DNNGuard [59] is one example that relies on a separate dedicated classifier for adversarial detection, which also comes at a high cost.

Prior work such as [21] have shown that adding some amount of random noise to inputs can help DNNs correctly classify adversarial inputs. Recent work by Guesmi et al. [18] proposed using approximate computation to introduce a controlled number of error in the DNN inference to correct some of the adversarial input into valid classifications. The observation that these and other prior work has made is that some amount of alteration to the model or input tends to affect adversarial inputs more than benign ones.

In this paper we propose a new, lightweight adversarial correction and/or detection mechanism for image classifiers that relies on the compute errors introduced by undervolting (running a chip at a voltage that is slightly below its safe margin). Prior work has shown that DNNs tend to be resilient to the errors introduced by undervolting [51], [52] in an FPGA. In this work we perform a thorough characterization of the effects of undervolting errors on classification of both adversarial and benign inputs. We show that undervolting errors during inference leads classifiers to assign a different class to adversarial images than would be assigned in the error-free inference. The new classification is either the correct class for the input (before the attack) or is a third class that is neither the original or the intended target of the attacker. We also show that undervolting is much less likely to lead to the misclassification of benign (unaltered) images. Based on these empirical observations, we propose a lightweight, energy efficient defense mechanism targeted at deployment on energy constrained edge devices.

Our proposed solution uses undervolting to achieve two goals: (1) introduce random errors caused by low-voltage operation into the DNN inference execution and (2) save energy by operating at the lower voltage.

Prior work has shown that errors introduced by undervolting are both random (they occur in random locations in different chips) and repeatable (they occur in the same location within

a chip) [3], [43]. The random distribution makes the defense unique to each chip, making it harder for an attacker to generate a successful general attack. The repeatably of the errors allows for system control over the approximate error rate that a chip is likely to encounter, allowing chips to continue execution without system crashes, in the presence of occasional localized errors. Prior work has used such controlled errors in security, for example, as a mechanism for hardware-backed authentication [4] or to attack SGX secure enclaves in Intel processors [43]. We propose using the same controlled errors to inject noise in the processor while running a DNN classifier.

We investigate two possible designs: one focused on adversarial correction, the other focused on detection. In the correction-based mechanism the system lowers supply voltage to a pre-determined set point, known to induce a certain number of errors, while the system is running the inference process. We show that this very simple approach leads the classifier to correctly classify an average of 50-55% of adversarial inputs, generated with multiple attacks. The defense mechanism compares the classification outcome for an error-free reference run with the undervolted run. If they are different, the input is classified as adversarial. Detection rate averages between 80% and 95% for a range of attacks.

We also developed a lightweight on-device training process that fine tunes the model to the error profile on each device. This process improves the classification accuracy for benign (non-adversarial) inputs in the presence of undervolting errors, while keeping the correction/detection rates of adversarials largely unchanged. Finally, we show that the proposed defense is resilient against attacks that have knowledge of the defense and attempt to circumvent it by training on a model with random errors or a fixed error distribution.

We evaluate the proposed system with an FPGA implementation of a DNN accelerator (which we undervolt with an external controller) as well as an error-model based software implementation that allows us to measure the impact of multiple error distributions and rates. We evaluate 10 attacks or attack variants on two popular deep convolutional neural networks, VGG16 [56] and DenseNet [22], on the ImageNet and CIFAR datasets.

Overall this paper makes the following contributions:

- The first work we are aware of to propose using undervolting errors as a defense against adversarial attacks on DNN classifiers.
- Proposes a lightweight on-device training mechanism to improve accuracy of benign inputs under errors.
- Performs a thorough study on the effects of different error rates and distributions on the adversarial detection/correction rates as well as the effects on accuracy of benign classification.
- Evaluates the proposed system on a FPGA platform and using software-based model.

The rest of this paper is organized as follows: Section II presents background and related work. Section III details the threat model. Section IV presents the details of the proposed

defense. Sections V and VI present the evaluation and Section VII concludes.

II. BACKGROUND AND RELATED WORK

A. Undervolting

Voltage undervolting is a common power saving approach, whereby reducing the supply voltage causes a significant reduction in power consumption. A large body of work [3], [13], [30] has explored approaches to dynamically reduce voltage margins to current operating conditions, in a process generally referred to as "undervolting." For example, the well-known Razor [13] design dynamically lowers supply voltage until occasional timing errors occur. Additional latches running on a delayed clock are used on the vulnerable paths to detect and recover from these errors. Other work by Lefurgy et al. [30] uses hardware critical path monitors specially built into the chip to detect when the processor approaches its timing margin as a result of undervolting. Salami et al. [51], [52] studied the effects of aggressive voltage undervolting of FPGA-based CNN accelerators with reduced supply voltage capability. They also provide experimental analysis of undervolting below the safe voltage, which leads to observable faults that manifest as bit flips. Similar studies have been performed by undervolting various system components in CPUs [3], [44], [23], [5], GPUs [31], DRAMs [9] which mainly focuses on fault characterization, voltage guardband analysis and fault mitigation.

B. Adversarial ML Attacks

Szegedy et al. in [58] showed that small perturbations to the inputs can force machine learning models to misclassify. Most attacks follow the same general approach. Let f be a probabilistic classifier with logits f_y and let $F(x) = \arg \max_y f_y(x)$. The goal of the adversary is to find an L^p -norm bounded perturbation such that $\Delta x \in B_\epsilon^p(0) := \{\Delta : \|\Delta\|_p \leq \epsilon\}$, where ϵ controls the attack strength, such that the perturbed sample $x + \Delta x$ gets misclassified by the classifier $F(x)$. The attackers problem formulated as:

$$\text{given } x, \text{ find } x' \text{ s.t. } \|x' - x\|_p \leq \epsilon_{max} \text{ and } F(x') \neq y \quad (1)$$

in case of *targeted* attacks adversary's goal is for x' to be misclassified as $F(x') = t$ which $t \neq y$ is a particular class other than y .

FGSM [15] proposed fast simple and efficient method for generating adversarial attacks by the L_∞ norm that uses the gradient of the loss with respect to the input data, then adjusts the input data to maximize the loss. **The Carlini-Wagner (CW)** attack differs from prior attack formulations in several ways, which allows it to find adversarial examples with considerably smaller perturbation amounts and higher accuracy. CW has variants for the L_0 and L_∞ distortion metrics. Both L_0 and L_∞ are not fully differentiable; accordingly, iterative algorithms are employed to find a solution. CW- L_0 uses the CW- L_2 attack to identify pixels which do not contribute much to the classifier output and freezes those pixel values. CW- L_∞ revises the objective function to limit perturbations to be less

than a threshold, iteratively searching for the smallest possible threshold. The **EAD** attack [10] formulates the objective function in terms of regularized elastic-nets, incorporating the L_1 distance metric for distortion, where elastic-net regularization is a linear mixture of L_1 and L_2 penalty functions. EAD has two variants, where the optimization process can be tuned by two different decision rules: *EN*, the elastic-net loss or L_1 , the least L_1 distortion. **DeepFool** [42] proposed a method to generate adversarial by searching for the closest distance from benign image to the decision boundary of the target image.

C. Defensive Techniques

Current Defense methods against adversarial attacks can be divided into the following broad categories:

1. Making the network itself robust [60], [45], [37], [27] by hardening the model, for example, by using *Adversarial Training*. The training set can be augmented with adversarial samples so that the network learns to classify adversarial samples correctly. However, this defense relies on known attacks and is difficult to generalize [45].

2. Transforming the input samples [32], [57], [62] which pre-processes the model inputs, such as by encoding or filtering, to denoise the adversarial perturbation.

Prior work has also attempted to detect adversarial inputs. Approaches proposed by [62] aim to "squeeze" an input image and [12] applies weighted dropouts to neurons, to detect an adversarial sample. Grosse et al. [17] proposed a statistical test using maximum mean discrepancy and suggests the energy distance as the statistical distance measure for detecting adversarials. Other approaches like [17], [39] suggest training a detector using adversarial examples.

In general, methods that rely on re-training are not generalizable. Detection approaches are more successful, but their overhead is generally very high. For instance, Feature Squeezing [62] has a 3-4 \times overhead because it relies on 4 models for detection. Our proposed solution is lightweight and highly effective at detecting a wide variety of adversarial attacks, including some of the strongest state-of-the-art attacks, like the CW-variants and EAD [53], [54].

III. THREAT MODEL

This paper assumes adversaries that have complete access to the DNN model, with full knowledge of the architecture and parameters, and are able to train their attacks accordingly. We assume an adversary that is able to directly deliver inputs to the DNN classifier, such as in [14], [48], [49] where attackers generate visual adversarial perturbations that are supposed to mimic real-world obstacles or create adversarial traffic signs to attack autonomous driving. We focus mainly on recent state-of-the-art optimization-based attacks—CW and EAD—since it has been demonstrated that all earlier attacks can be overcome utilizing other methods, such as adversarial training [15] or defensive distillation [46], which could be used in combination with our approach. Finally, our defense is targeted at edge devices such as smartphones or autonomous vehicles, rather than server or cloud-based classifiers.

IV. DEFENSE DESIGN

Lowering the supply voltage of chips leads to significant power savings. However, reduced voltage operations may also introduce some faults in the device. This is because propagation latency increases at lower supply voltages, which can lead to timing faults. These timing faults can manifest as bit-flips in logic outputs or memory. This can cause most applications to crash. DNNs are known to be resilient to some errors, generally experiencing a graceful degradation in accuracy. In worst-case, if the system is undervolted aggressively below a critical region, it may cause a system crash.

A. Using Undervolting as a Defense Mechanism

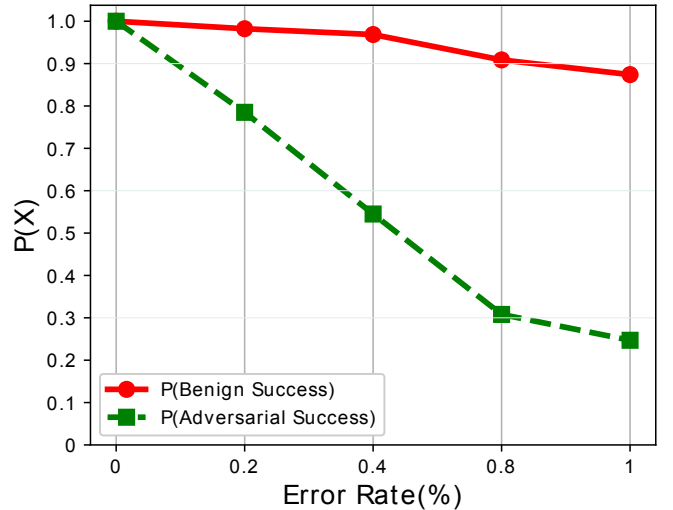


Fig. 1: Probability of success for benign vs adversarial classification under the effects of random errors/noise in a DNN model.

It has been shown [11], [20], [29] that adding some amount of random noise to images can help DNNs correctly detect adversarial inputs by lowering their success rate more compared to the benign counterpart. However, the key observation we make in this work is that injecting noise directly in the model improves the ability to detect stronger adversarial inputs, for which correct classification cannot be achieved.

Figure 1 shows the response of a DNN classifier to increasing levels of random noise injected into the model, while classifying both adversarial and benign inputs. We can see that, as the error rate increases the adversarial inputs are less likely to be classified in the intended adversarial class, with their probability of success dropping steeply. Benign inputs are also affected but to a much smaller degree.

We propose using the errors introduced by controlled undervolting of a chip to introduce sufficient perturbations to the model to disrupt adversarial inputs. The proposed system is deployed in three main phases, shown in Figure 2, as follows:

B. Phase I: Offline Device Characterization

In general, the voltage spectrum of a device can be classified into three regions: *Safe*, *Critical* and *Crash*. In the *Safe* region,

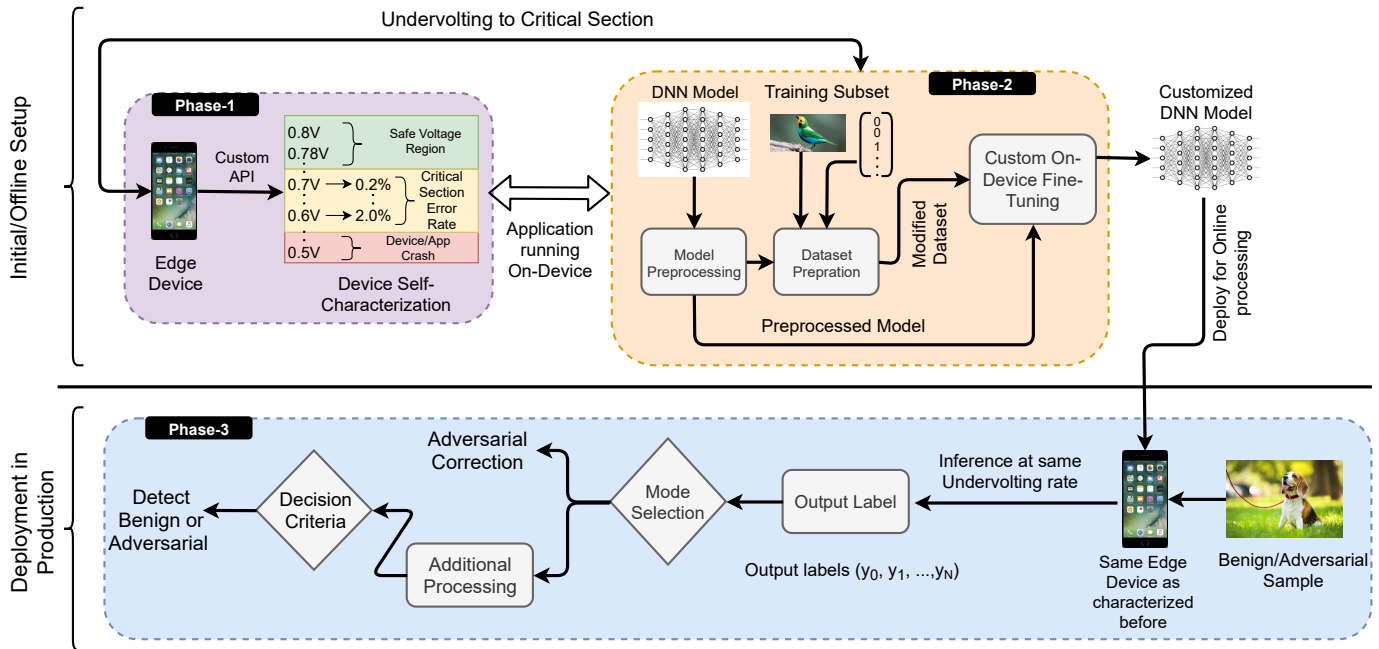


Fig. 2: Global flow of the proposed design. Based on the user-provided constraints, we output the best defense layout customized for the resource-constrained target hardware platform.

the device operates normally, with no errors. In the *Critical* voltage region the chip will experience occasional errors. Depending on the system and/or application they may continue to operate in the presence of these errors. Finally, the *Crash* voltage is too low for the system to operate. Our defense utilizes voltages in the *Critical* range.

Manufacturing process variation makes the response of each device to undervolting unique. As a result, the critical region resides at different voltage ranges for each chip. The target device therefore needs to be programmed to characterize these regions after manufacturing. This characterization can be performed by either the chip or device manufacturer, and it involves progressively lowering the supply voltage and running a built-in self test application designed to detect compute or memory errors. Figure 3 illustrates this process. Based on the different fault or error rates profiled, the device can now be undervolted to a fixed voltage supply in the critical section, which will be used for the rest of the offline processing and online execution.

C. Phase II: At Setup On-device Tuning

Our analysis shows that the accuracy of the classification of benign inputs can also be affected by undervolting. To reduce this impact we develop a lightweight on-device fine-tuning process to refine the model to account for errors. This solution takes advantage of the fact that undervolting errors occur in the same functional units. In accelerator designs that use mostly static mapping of computation to hardware, this means that errors affect mostly the same model nodes across runs. Fine-tuning the *pre-trained* classifier model in the presence of errors allows the model to adapt and recover most

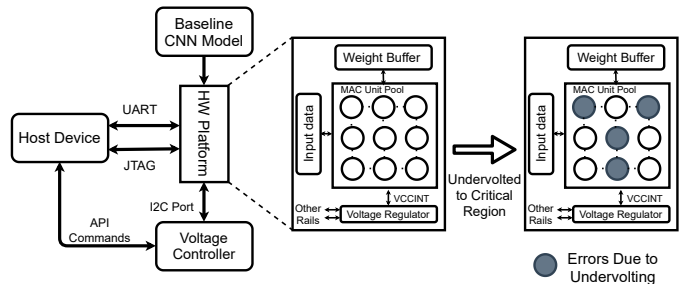


Fig. 3: Hardware Platform overview with undervolting.

of the accuracy loss. An important constrained on the fine-tuning process is to keep its overhead very low, given that it needs to run on relatively less powerful edge on-devices. This means the fine-tuning needs a minimized training set, assuring low storage and communication overhead, as well as the number of training iterations.

Given these constraints, a small subset of less than 0.6% set is sampled randomly from the full training dataset. The benefit of choosing such a small set is that it takes fewer resources and time than using the whole dataset to re-train, allowing deployment on resource-constrained devices like smartphones. Since the training subset is small, the number of training epochs can be much smaller to prevent model overfitting.

1) *Model Preprocessing*: Modern CNNs consist of a Softmax layer which is often used as the last activation function of a neural network to normalize the output vector Z produced by the last hidden layer of a CNN, called *logits*, to a probability distribution over predicted output classes. A single unit of a

standard softmax function is denoted as:

$$\sigma_i = \frac{e^{z_i/T}}{\sum_{j=1..N} e^{z_j/T}}$$

where $Z = (z_1, z_2, \dots, z_N)$, are the N logit outputs corresponding to N classes in the dataset and T denotes the *temperature* parameter. Generally, the T value is set to 1 producing a discrete distribution between 0 and 1. We set T to a higher value in order to increase the uncertainty in the probability distribution vector leading the vector components to converge towards $1/N$. The softmax layer in the *pre-trained* model is modified with a custom softmax activation function. The value of T is model specific and can be refined along with other parameters such as learning rate, step size and number of epochs, to achieve fast and accurate fine-tuning without overfitting.

2) *Dataset Processing*: A small training dataset is required for fine-tuning. The dataset selection and processing is highlighted in Step 1 of Figure-4. A training set consists of (X, Y) tuples where $X=(x_0, x_1, \dots, x_K)$ denote K input samples/images and $Y=(y_{1i}, y_{2i}, \dots, y_{Ki} \mid i = 1, 2, \dots, N)$, denote N class labels for each of the K inputs. The values for these N class labels are binary, with only the correct class having a value of 1 and the rest are 0. The idea of this step is to use the class probability vectors produced by the softmax layer containing the probability of each class for an input example, also denoted as *soft labels* instead of using the discrete-binary or *hard* class labels to fine-tune the model. Using the probability vectors as the Y values are beneficial as they contain additional information about each class instead of simply providing the correct class label. The intuition here is that when a model is being trained, the knowledge is encoded in both the weight parameters and the probability vectors. Hence using the *soft* labels helps extract the class knowledge acquired from these probability vectors.

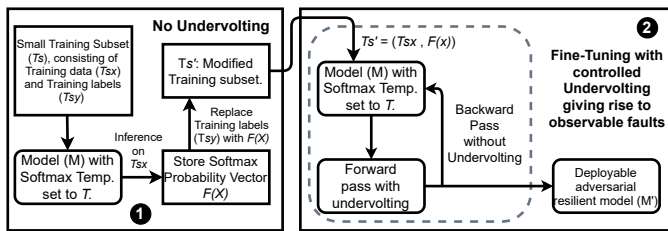


Fig. 4: Dataset preparation and fine-tuning flow.

The second fine-tuning step is 2 in Figure 4. The targeted chip is undervolted during in order to surface the hardware errors and their effect on the model under training. The intuition is that since the error distribution does not change significantly over time, the model can adapt to this distribution sufficiently to recover the classification accuracy for benign inputs while the success rate of an adversarial inputs remains lower. The processed pre-trained model is fine-tuned with the modified dataset under errors. For a model M with features θ

and a given set of sample $(x, P(x) \mid x \in X)$, where x is the input sample, and $P(x)$ are the soft labels, the goal of this phase is to solve the following optimization problem:

$$\arg \min_{\theta} -\frac{1}{|X|} \sum_{x \in X} \sum_{i \in N} P_i(x) \log M_i(x)$$

This means for each sample $(x, P(x))$ we consider the log-likelihood $L(M, x, P(x))$ of model M on $(x, P(x))$ and average it for the training set X .

The fine-tuning process involves two passes. The forward pass predicts the output class labels based on some input data. In the backward pass the predicted output is compared with the actual target output. The loss is calculated for that iteration, and is used to update the weights and biases accordingly. The process repeats until it reaches the iterations limit or when the model achieves a threshold accuracy. In our design only the forward pass is undervolted, while the backward pass is performed at nominal voltage to ensure error-free backpropagation of updated parameters. Figure 5 illustrates this process. Once the fine-tuning is complete, the updated model is ready to be deployed in production.

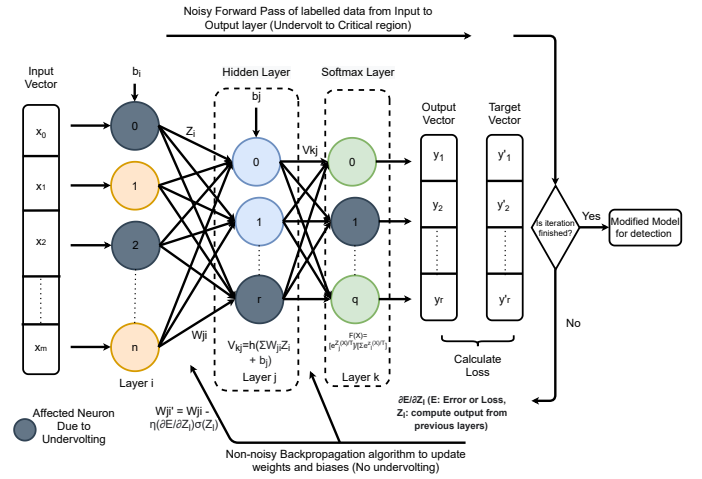


Fig. 5: Detailed custom fine-tuning flow.

D. Phase III: Runtime Adversarial Correction/Detection

The final phase of our proposed design consists of the deployment of the modified model in the defense mechanism. We examine two designs, with different effectiveness and overhead tradeoffs: (1) adversarial correction, which accurately classifies a subset of the adversarial inputs with no performance overhead and lower energy than the baseline, and (2) adversarial detection, which detects $>90\%$ of adversarial inputs at the cost of higher performance overhead. We describe the two approaches as follows:

1) *Adversarial Correction*: The goal of a model or a classifier m , having logit values as k_y , can be given as $F(x) = \arg \max_y k_y(x)$, where x is an input to the model m . Now, for an adversarial that has been perturbed from the original input x as $(x + \Delta x)$, the goal for an adversarial correction can be summarized as, $F(x + \Delta x) = y = F(x)$, where $y \in (1, \dots, K)$,

denoting the class labels. By simply running the fine-tuned model on an undervolted chip, the associated errors will induce the classifier to correctly classify a majority of the adversarial inputs. ① in Figure 6 shows the general flow for this method. This approach has no performance overhead and, because of undervolting, has lower energy than the unprotected baseline. However, the correction rate is only around 50-60% of the adversarial inputs we test.

2) *Adversarial Detection*: In order to detect if an input is benign or adversarial, our approach compares the classification output of a reference inference pass at nominal voltage with an undervolted inference pass for the same input. In the first pass, a model with the same characteristics and hyperparameters as the baseline model is selected to get the classification result for the input example *without* any undervolting. In the second pass, the modified model is used to get the classification result, *with* undervolting to the same critical voltage used during fine-tuning of the model. Both these inference results are compared, and if the results match, the input image is labeled as legitimate otherwise, it is flagged as adversarial. ② in Figure 6 illustrates this technique. The intuition behind this approach is that undervolting is more likely to change the classification (relative to reference run) for the adversarial inputs. Benign inputs are less likely to be affected and their classification will match with the reference. We show that this approach is 80-90% effective at detection adversarial inputs. However, because it requires an error-free reference run, this approach doubles the inference latency – although the energy overhead is only about 70% due to the undervolting power savings.

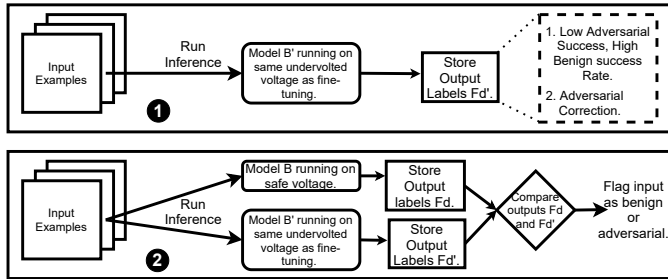


Fig. 6: Runtime adversarial correction/detection mechanism.

V. METHODOLOGY

A. Evaluation platform

We utilize CHaiDNN [61], a Deep Neural Network library for acceleration by Xilinx as our hardware platform for evaluation. CHaiDNN is freely available and is a fully integrated platform to accelerate deep neural networks on Xilinx UltraScale MPSoCs. It supports most of the widely used CNNs and has the ability to add custom networks and layers.

B. FPGA Platform

We deploy CHaiDNN on the Xilinx Zynq Ultrascale+ ZCU104 FPGA platform [2]. The board consists of the

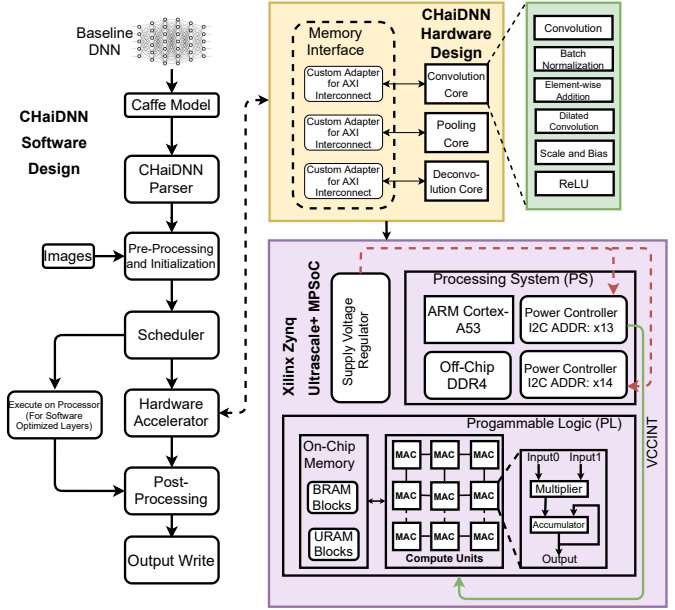


Fig. 7: CHaiDNN baseline accelerator design on ZCU104 platform.

XCZU7EV-2FFVC1156 MPSoc. The Processing System (PS) of the device consists of a quad core Arm Cortex-A53 applications processor (APU), a dual-core Cortex-R5 real-time processor (RPU). It is also equipped with a graphics processing unit and fabricated with a 16nm FinFET+ programming logic. The Programmable Logic (PL) part features about 504K LUTs, 11Mb of Block RAM (BRAM), 27Mb of UltraRAM (URAM), 1728 DSP slices. The board is also equipped with a 2GB 64-bit DDR-4 off-chip memory.

C. Datasets and Classifier Models

We evaluate our defense on two popular convolution-based deep neural networks datasets and models:

1. **CIFAR-10 on DenseNet**: The CIFAR-10 [24] dataset consists of 60,000 32x32 color images in 10 classes, with 6,000 images per class. There are 50,000 training images and 10,000 test images. We use a DenseNet [22], [38] model to evaluate the CIFAR-10 dataset. DenseNet (Figure 8) is composed of an initial convolution layer followed by Dense and Transition blocks and a softmax classifier. In the Dense Blocks (DB), the layers are densely connected.

2. **ImageNet on VGG16**: The ImageNet [26] project is a large visual database designed for use in visual object recognition software research. The most highly-used subset of ImageNet is the ImageNet Large Scale Visual Recognition Challenge (ILSVRC) [50] image classification and localization dataset. This dataset spans 1,000 object classes and contains 1,281,167 training images, 50,000 validation images and 100,000 test images. We use the VGG16 [56] (Figure 8) model to evaluate for ImageNet dataset. It consists of 16 convolution layers, with activation layers in between, followed by 3 fully connected layers and a softmax layer for classification.

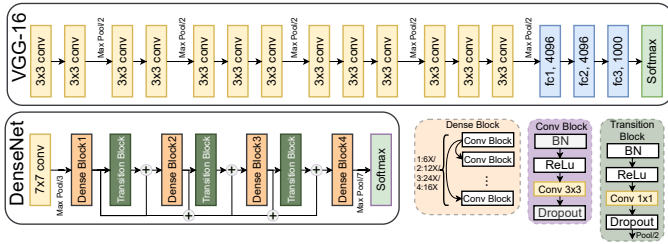


Fig. 8: VGG-16 and DenseNet model architecture.

TABLE I: Adversarial attack evaluation summary.

Dataset	Attack	Mode	Params	Success rate	Prediction Conf.	Distortion		
						L_0	L_2	L_∞
ImageNet	FGSM	-	eps=0.0040	99%	63.9%	94%	3.1	0.008
	CW _{L0}	LL	k=5	100%	84.4%	42.4%	13.65	0.96
		Next	k=5	97%	92.9%	42.2%	10.44	0.94
	CW _{L2}	LL	k=5	97%	75.25%	54.3%	1.027	0.031
		Next	k=5	90%	76.3%	32.2%	0.66	0.019
	CW _{L∞}	LL	k=5	100%	91.8%	99.9%	3.05	0.01
		Next	k=5	100%	94.7%	100%	2.27	0.01
	Deepfool	-	-	-	100%	79.59%	98.4%	0.726
EAD _{L1}	LL	k=10	-	100%	100%	54.7%	3.56	0.29
	Next	k=5	-	100%	-	-	-	-
CIFAR-10	FGSM	-	eps=0.0040	100%	84.85%	99.7%	0.863	0.016
	CW _{L0}	LL	k=5	100%	97.60%	2.4%	2.530	0.712
		Next	k=5	100%	98.19%	1.9%	2.103	0.650
	CW _{L2}	LL	k=5	100%	97.35%	85.5%	0.358	0.042
		Next	k=5	100%	97.90%	76.8%	0.288	0.034
	CW _{L∞}	LL	k=5	100%	97.79%	99.5%	0.527	0.014
		Next	k=5	100%	98.22%	99.0%	0.446	0.012
	Deepfool	-	-	-	98%	73.45%	99.5%	0.235

D. Input Dataset, Attacks

We evaluate our defense on all of the attacks mentioned in Table I. We use two untargeted attacks: FGSM, Deepfool and four targeted attacks: CW_{L0} , EAD_{L1} , CW_{L2} , $CW_{L\infty}$. For each targeted attack, we deploy two different targets, both of which aim to misclassify an input into a target class. The *least-likely*(LL) class; $t = \min(y)$ and the *Next* class; $t = L + 1 \bmod \#classes$. Here, t is the target class, L is the sorted index of top ground truth classes, and y is the prediction vector of an input image. We select a total of 1,000 legitimate samples and 100 adversarial samples for each attack method from each of the two dataset.

E. Undervolting methodology

We perform undervolting characterization on the FPGA device using an external voltage controller, the Infineon USB005, which is connected to the board using an I2C cable. The provided PowerIRCenter GUI enables us to read and write the different voltage rail supplies to the board. For this study, we focus on VCC_{INT} voltage rail accessible using PMBus address 0x13 with a supply voltage of 0.852V. This voltage rail controls some of the internal components in PS and, most importantly, the DSP, LUT units in PL. We can also monitor the power consumption of the voltage rails and the temperature using this GUI. We layout our setup in Figure 9(a).

We notice when undervolting this device between the critical region, we sometimes get an application crash. We attribute the reason for this to be the shared voltage rail in ZCU104, between the Processing System and Programmable logic units. Undervolting more causes a device crash. Given this scenario, we inject errors directly in the Multiply-Accumulate (MAC)

units of the CHaiDNN hardware since these are the dominant component of the accelerator in terms of FPGA resource utilization. Our design deploys 256 such MAC units. They are also the functional units more heavily utilized by the CNN models and we expect undervolting to primarily affect MAC units. We simulate this effect in the ZCU104 device using CHaiDNN and compute the accuracy loss on a test set with different error rates introduced.

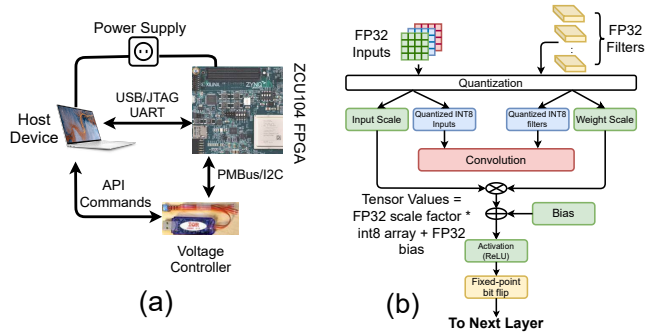


Fig. 9: (a) Hardware platform setup and (b) Software model flow.

F. Software Simulation and Quantization

Since the CHaiDNN accelerator does not support training or fine-tuning, we evaluate the error injection and on-device fine-tuning on an Intel Core-i7 CPU@3.40GHz CPU using TensorFlow version 1.14 [1]. We simulate the behavior of model computation exactly as in CHaiDNN. We inject errors after every convolution layers of the model which includes activation functions, in the software. The same holds true in case of CHaiDNN where the convolution operation itself, along with the activation function, are computed using the 256 MAC units. We also quantize the input and the weights to a fixed INT8 precision and then convolve them, followed by bias addition and activation. The reason for quantizing the inputs and weights is to match the CHaiDNN INT8 computations on the MAC units. The errors are injected as bit flips after every convolution layer. Figure 9(b) illustrates the error model and quantization process.

This model is next fine-tuned following the same logic and flow shown in Figure 5. The error distribution is normal and random, with the final results are averaged for multiple such distributions. To validate this simulation, we compare the accuracy loss due to undervolting effects on our FPGA platform running the accelerator and the software implementation on a sample benign test set. Figure 10 shows the effects of undervolting the VGG16 model on the FPGA accelerator and in the software. We can see that classification accuracy as a function of the error rate introduced matches very well in the software model with the FPGA-based injection, across three different error models (single-bit error, 25% bit flips and 50% bit flips). Hence with some calibration, it allows us to replicate the effects of undervolting in the software platform and use it to evaluate the custom fine-tuning as well as conduct sensitivity studies with respect to error rates.

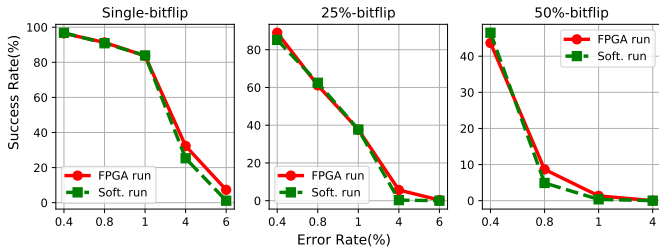


Fig. 10: Undervolting effects on FPGA vs software.

VI. EVALUATION

A. Adversarial Detection and Correction

Figure 11 shows the detection and the correction rates for each adversarial attacks under different simulated error rates for ImageNet and CIFAR-10 examples respectively. Our error model assumes, in this case, that 50% of the bits in each affected output are flipped.

The error rate in the model will vary with the rate of undervolting, affecting the adversarial detection rate, which improves as the rate of error introduced in the model increases. For instance, with a 2% error rate, the average detection rate is at 97% compared to 81% with a 0.02% error rate in the Imagenet dataset. Adversarial correction is evaluated based on the predicted labels of the adversarial examples and comparing the Top-K of these labels with the ground truth of that adversarial. We show Top-1, and Top-5 correction rates for the ImageNet dataset and just Top-1 for CIFAR-10 since the latter only has 10 class labels compared to 1,000 class labels in ImageNet. Figure 11 indicates our defense mechanism is highly effective at reducing the success rate across multiple, diverse adversarial attacks.

As expected, accuracy for the benign inputs decreases with the increase in error rate. However, the effect of the errors on benign inputs remains modest. The benign *True Positive Rate (TPR)* reaches a low of 80% for 2% error rate. At the same time, it is above 90% for lower error rates at which adversarial detection rates exceed 95%. Fine-grain undervolting allows some control over the error rate. This enables the system to trade-off benign accuracy for adversarial detection rate, to adapt to the needs and constraints of the application.

B. The Benefits of On-device Fine-tuning

Figure 12 and 13 highlights the contributions of on-device fine-tuning to the model accuracy and adversarial detection rate. We show three designs, with classification accuracy for benign inputs and detection/correction for adversarial inputs at different error rates. Adversarial results are averaged across all the attacks we study.

1) *Undervolt*: This technique is the core of our design. We evaluate the different models and datasets using just undervolting, with no fine tuning. We study how these errors affect the accuracy of the benign inputs and the success rate for different adversarial inputs. For benign examples, we notice that the model’s accuracy is quite high for low error rates.

However, at high error rates the accuracy drops to almost 0%. This shows that undervolting alone is only feasible at low error rates, where the adversarial detection rate is less than 80%.

2) *Undervolt + Regular Fine-Tuning (RFT)*: This technique involves fine-tuning of the model with a small dataset. In this case, fine tuning does not employ the distillation process described in Sec IV. We observe that fine-tuning improves benign accuracy significantly at high error rates. For the ImageNet dataset with a higher error rate of 2%, the benign TPR increases by 98.5% to 80%, and there is a 34.4% average increase across all error rates. There is also a 3.26x increase in average Top-1 correction rates for ImageNet and a 2.33x increase for CIFAR-10 adversarial vs. undervolting alone.

3) *Undervolt + Custom Distillation-based Fine-Tuning (CDFT)*: This technique adds distillation to fine-tuning and represents our main proposed solution. In CDFT, we incorporate a modified defensive distillation strategy to bring down the success rate of the adversarials. CDFT is particularly effective at lower error rates and complements undervolting well. For instance, in ImageNet with a 0.02% error rate, we see a 51% increase in detection rate for adversarials compared to fine-tuning alone. This result is interesting since low error rates mean the accuracy of benign images are higher, thus achieving a high detection rate of 90.1% overall, averaged across all error rates (Figure 13 (Top)).

C. Sensitivity to Error Profile

We investigate the effect of different error profiles on the effectiveness of our design. We model single bit errors as well as multi-bit errors covering 25% and 50% of the bits in a word. We expect undervolting to produce multi-bit errors, and therefore use 50% bit flips in our main results. For completeness, however, we include results for single bit errors as well as 25% bit errors.

Figure 14 shows the average detection and correction rates for the three error profiles. We show results for three different thresholds for benign accuracy: >80%, >85% and >90%. For each experiment we use the lowest error rate that is sufficient to ensure the benign accuracy threshold is met. We can see that the correction and detection rates are remarkably consistent across different error profiles for both ImageNet and CIFAR data sets. The detection rates varies by at most 4% between different rates of bit flips and when considering a benign threshold TPR of greater than 90% for both the datasets.

Tables II shows a summary of the detection and correction rates across all attacks and error profiles we evaluate for the ImageNet dataset. For each error profile, we use an error rate that is sufficient to achieve a >85% benign TPR for the main defense (Undervolt+CDFT).

D. Comparison with Prior Work

We compare our defense with Feature Squeezing (FS) [62], a defense that manipulates, or “squeezes”, input images (for example by reducing the color depth and smoothing to reduce the variation among pixels). If the low-resolution image produces substantially different classification outputs

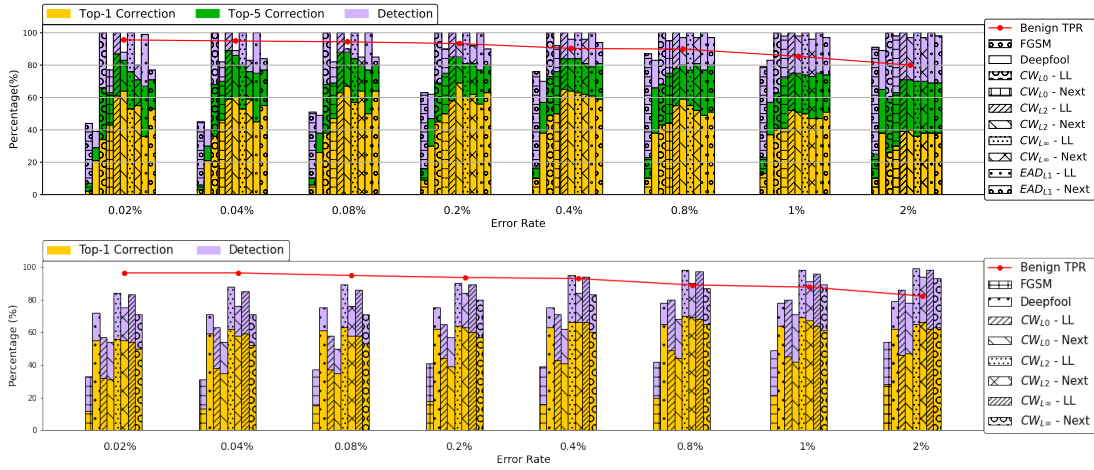


Fig. 11: Benign TPR, adversarial detection and correction for different error/fault rates in ImageNet (Top) and CIFAR-10 (Bottom).

TABLE II: Detection/Correction rate of various attacks based on different evaluation techniques, for ImageNet dataset.

Bit flips	Technique	Benign TPR(%)	L_0 attacks		L_1 attacks		L_2 attacks			L_∞ attacks		
			CW		EAD		Deepfool(%)	CW		FGSM(%)	CW	
			LL(%)	Next(%)	LL(%)	Next(%)		LL(%)	Next(%)		LL(%)	Next(%)
Single ^a	Undervolt	25.3	100/5	100/7	100/5	100/8	98/8	100/6	100/9	87/1	100/4	100/9
	Undervolt+RFT	89.3	100/51	92/51	100/53	88/61	64/37	100/67	96/63	67/8	100/62	96/60
	Undervolt+CDFT	85.42	100/52	93/57	100/62	95/62	79/41	100/66	98/69	79/12	100/66	97/63
25%	Undervolt	62.5	100/12	89/22	98/15	88/26	78/18	100/27	93/30	1/5	100/30	89/19
	Undervolt+RFT	91.2	100/39	82/51	98/45	85/59	59/26	100/57	93/59	48/5	100/64	88/55
	Undervolt+CDFT	87.6	100/43	89/52	100/54	91/59	66/33	100/57	95/60	63/9	100/59	91/58
50%	Undervolt	77.4	100/13	91/19	100/16	93/17	85/17	100/23	93/28	59/4	100/19	97/25
	Undervolt+RFT	93.04	100/48	87/53	100/57	86/58	58/27	100/73	95/69	53/5	100/64	92/60
	Undervolt+CDFT	89.89	100/49	92/51	100/61	94/59	76/38	100/65	96/66	70/10	100/63	96/62

^aThe benign threshold is set to 85% on the final technique (Undervolt+CDFT). For Single bit flip section, we achieve 85.42% Benign TPR at a 4% error rate, hence the other techniques in that section are calculated based on the same error rate. Similar convention is followed for the rest of the sections in this Table.

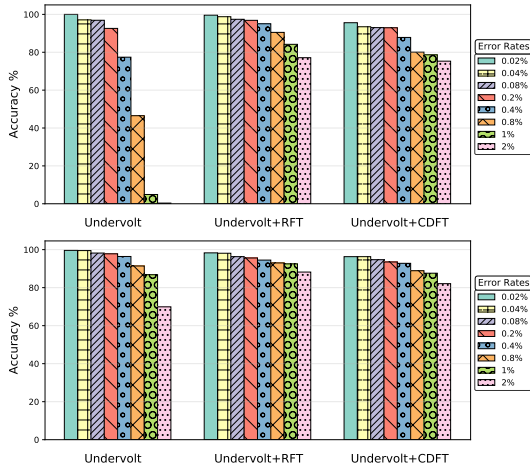


Fig. 12: Benign Examples on ImageNet(Top) and CIFAR-10(Bottom).

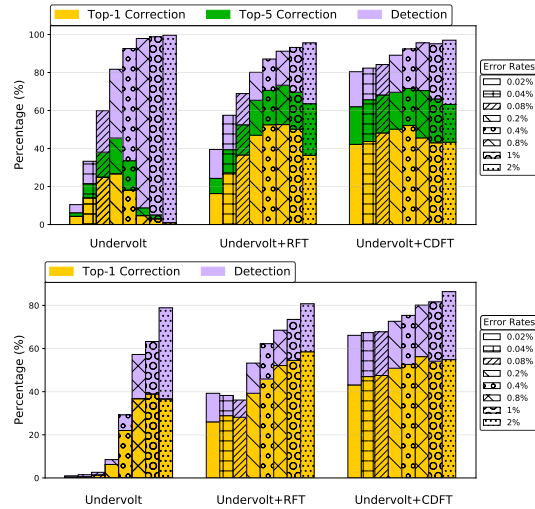


Fig. 13: Adversarial Examples on ImageNet(Top) and CIFAR-10(Bottom).

than the original image, the input is likely to be adversarial. FS combines multiple squeezers for detection resulting in higher performance overhead than our proposed technique. We applied FS to our set of Adversarial images for both ImageNet and CIFAR-10. Figure 15 compares the average adversarial detection rate of FS and our defense for different error rates. We observe that our design compares favorably to FS, even

for low error rates. As the error rate increases, our technique performs better, reaching a 97% adversarial detection rate.

We also observe that FS can complement our defense to achieve higher detection rate. Table-III shows detection rates for a FS variant (using a 2x2 median filter smoothing) compared to our main design (Undervolting+CDFT) and to our

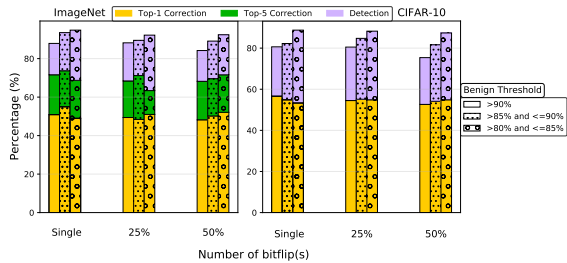


Fig. 14: Adversarial detection and correction based on varying bit flips and different benign TPR thresholds.

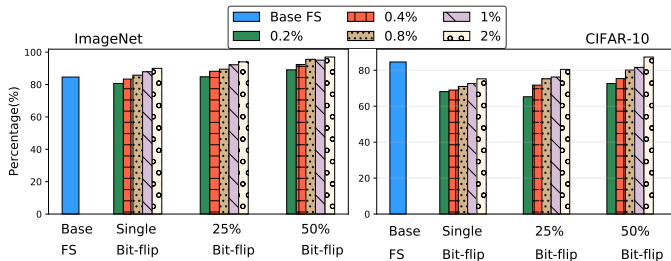


Fig. 15: Comparison with Feature Squeezing based adversarial detection rate.

design that includes FS (Undervolting+CDFT+FS). We can see that the combined design achieves the highest detection rate for both datasets, demonstrating that undervolting can potentially complement other defenses. However, we do note that the benign TPR decreases slightly for the combined technique. Additional tuning of the combined design might be needed, but was beyond the scope of this work.

E. Resilience to Defense-aware Attacks

We evaluate our solution against attackers that are aware of the details of our defense. We examine two such attacks:

1) *Attack Trained under Random Noise*: In the first attack we assume the adversary is aware of the error-based defense, but has no access to the victim’s hardware (Figure 16 ①) and does not know the error distribution profile of the victim’s device. The attack adds random noise into the model during adversarial construction to attempt to circumvent our defense.

2) *Attack Trained on Device*: In the second scenario, we assume an attacker with full control of a hardware platform that includes our defense, but is not the device under attack. Control of the device allows the attacker to learn the error distribution of the platform, the model parameters, and can use it indefinitely to create adversarial attacks directly, as shown

TABLE III: Comparison of average adversarial detection rate using a fixed benign TPR threshold for ImageNet/CIFAR-10.

Technique	Benign TPR(%)	Detection(%)
FS(2x2)	93.80/93.20	79.40/85.40
U+CDFT	92.93/93.50	85.20/81.25
U+CDFT+FS(2x2)	90.40/91.70	91.60/89.50

in ② of Figure 16. The attack is constructed by training on a device with a pre-determined error profile. The goal of this exercise is to determine if an attacker that controls one device can successfully attack a different device, with different error characteristics.

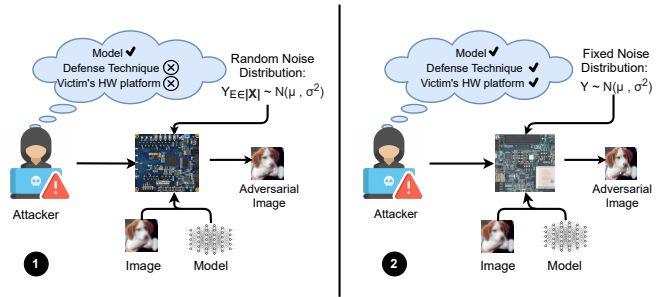


Fig. 16: Adaptive attack scenario.

We implement both defense-aware attacks on top of the CW_{L2} attack and use them to generate adversarials based on the ImageNet dataset. All generated adversarials have a baseline success rate of 100%. We re-evaluate these adversarials on a different simulated device with a different error profile. Table IV shows the detection rate for our design for different error rates. We can see that the detection rate for both attacks is very high. This shows that as long as the physical device is not compromised, the unique error characteristics of each device ensure a robust defense against defense-aware adversarials.

TABLE IV: Detection rates of adaptive attacks evaluated using ImageNet dataset.

Error Rate	Detection Rate for Random Noise Attack	Detection Rate for Fixed Error Attack
0.2%	88%	81%
0.4%	90%	88%
0.8%	96%	95%
1%	99%	98%
2%	100%	100%

F. Energy Impact

Finally, we evaluate the energy impact of the proposed defense, using measurements of power consumption and execution time performed on our FPGA-based implementation of ChaiDNN running VGG16. Table V shows inference energy for our defense relative to the unprotected baseline for both correction and detection. Due to the substantial power reduction achieved by undervolting and given that our correction method has no performance overhead, our correction defense achieves about 30% energy savings. Detection requires two sequential inference passes, but due to undervolting this comes at a 70% increase in energy cost instead of $2\times$.

VII. CONCLUSION AND FUTURE WORK

In conclusion, this paper proposes a novel defense against adversarial ML attacks that relies on undervolting. We show that the technique is highly effective, with $> 90\%$ detection

TABLE V: Relative energy for adversarial correction and detection with critical voltage in ZCU104 running CHaiDNN.

Critical Voltage	Relative Energy for Correction	Relative Energy for Detection
0.660V	0.716	1.716
0.656V	0.714	1.714
0.652V	0.670	1.670

rate of adversarial inputs for a variety of state-of-the-art attacks. The defense is also energy efficient, due to the power savings from low voltage operation. We also show how the randomness introduced by the unique device characteristics makes our approach robust against defense-aware attacks.

In future work we plan to extend our study to more types of devices with different characteristics, including other FPGA-based designs and GPUs.

REFERENCES

- [1] “Tensorflow,” <https://www.tensorflow.org/>. [Online]. Available: <https://www.tensorflow.org/>
- [2] “Zynq ultrascale+ mp soc zcu104 evaluation kit,” <https://www.xilinx.com/products/boards-and-kits/zcu104.html>. [Online]. Available: <https://www.xilinx.com/products/boards-and-kits/zcu104.html>
- [3] A. Bacha and R. Teodorescu, “Dynamic reduction of voltage margins by leveraging on-chip ECC in Itanium II processors,” in *International Symposium on Computer Architecture (ISCA)*, June 2013, pp. 297–307.
- [4] —, “Authenticache: Harnessing cache ECC for system authentication,” in *International Symposium on Microarchitecture (MICRO)*, December 2015, pp. 1–12.
- [5] R. Bertran, A. Buyuktosunoglu, P. Bose, T. J. Slegel, G. Salem, S. Carey, R. F. Rizzolo, and T. Strach, “Voltage noise in multi-core processors: Empirical characterization and optimization opportunities,” in *2014 47th Annual IEEE/ACM International Symposium on Microarchitecture*, 2014, pp. 368–380.
- [6] M. Bojarski, D. Del Testa, D. Dworakowski, B. Firner, B. Flepp, P. Goyal, L. D. Jackel, M. Monfort, U. Muller, J. Zhang *et al.*, “End to end learning for self-driving cars,” *arXiv preprint arXiv:1604.07316*, 2016.
- [7] X. Cao and N. Z. Gong, “Mitigating evasion attacks to deep neural networks via region-based classification,” in *Proceedings of the 33rd Annual Computer Security Applications Conference on*, 2017, pp. 278–287.
- [8] N. Carlini and D. Wagner, “Towards evaluating the robustness of neural networks,” in *IEEE Symposium on Security and Privacy (SP)*, 2017.
- [9] K. Chang, O. Mutlu, A. G. Yaglikçi, S. Ghose, A. Agrawal, N. Chatterjee, A. Kashyap, D. Lee, M. O’Connor, and H. Hassan, “Understanding reduced-voltage operation in modern dram devices: Experimental characterization, analysis, and mechanisms,” 06 2017, pp. 52–52.
- [10] P.-Y. Chen, Y. Sharma, H. Zhang, J. Yi, and C.-J. Hsieh, “Ead: elastic-net attacks to deep neural networks via adversarial examples,” in *Thirty-second AAAI conference on artificial intelligence*, 2018.
- [11] J. M. Cohen, E. Rosenfeld, and J. Z. Kolter, “Certified adversarial robustness via randomized smoothing,” *arXiv preprint arXiv:1902.02918*, 2019.
- [12] G. S. Dhillon, K. Azizzadenesheli, J. D. Bernstein, J. Kossaifi, A. Khanna, Z. C. Lipton, and A. Anandkumar, “Stochastic activation pruning for robust adversarial defense,” in *International Conference on Learning Representations (ICLR)*, 2018.
- [13] D. Ernst, N. S. Kim, S. Das, S. Pant, R. Rao, T. Pham, C. Ziesler, D. Blaauw, T. Austin, K. Flautner, and T. Mudge, “Razor: A low-power pipeline based on circuit-level timing speculation,” in *International Symposium on Microarchitecture (MICRO)*, December 2003, pp. 7–18.
- [14] K. Eykholt, I. Evtimov, E. Fernandes, B. Li, A. Rahmati, C. Xiao, A. Prakash, T. Kohno, and D. Song, “Robust physical-world attacks on deep learning visual classification,” in *Proceedings of the IEEE Conference on Computer Vision and Pattern Recognition*, 2018, pp. 1625–1634.
- [15] I. J. Goodfellow, J. Shlens, and C. Szegedy, “Explaining and harnessing adversarial examples,” *arXiv preprint arXiv:1412.6572*, 2014.
- [16] I. J. Goodfellow, J. Shlens, and C. Szegedy, “Explaining and harnessing adversarial examples,” in *ICLR 2015 : International Conference on Learning Representations 2015*, 2015.
- [17] K. Grosse, P. Manoharan, N. Papernot, M. Backes, and P. McDaniel, “On the (statistical) detection of adversarial examples,” 2017.
- [18] A. Guesmi, I. Alouani, K. Khasawneh, M. Baklouti, T. Frikha, M. Abid, and N. Abu-Ghazaleh, “Defensive approximation: Enhancing cnns security through approximate computing,” *arXiv preprint arXiv:2006.07700*, 2020.
- [19] K. He, X. Zhang, S. Ren, and J. Sun, “Deep residual learning for image recognition,” in *2016 IEEE Conference on Computer Vision and Pattern Recognition (CVPR)*, 2016, pp. 770–778.
- [20] Z. He, A. S. Rakin, and D. Fan, “Parametric noise injection: Trainable randomness to improve deep neural network robustness against adversarial attack,” in *Proceedings of the IEEE Conference on Computer Vision and Pattern Recognition*, 2019, pp. 588–597.
- [21] S. Hu, T. Yu, C. Guo, W.-L. Chao, and K. Weinberger, “A new defense against adversarial images: Turning a weakness into a strength,” in *NeurIPS 2019 : Thirty-third Conference on Neural Information Processing Systems*, 2019, pp. 1633–1644.
- [22] G. Huang, Z. Liu, L. van der Maaten, and K. Q. Weinberger, “Densely connected convolutional networks,” 2018.
- [23] M. Kaliorakis, A. Chatzidimitriou, G. Papadimitriou, and D. Gizopoulos, “Statistical analysis of multicore cpus operation in scaled voltage conditions,” *IEEE Computer Architecture Letters*, vol. 17, no. 2, pp. 109–112, 2018.
- [24] A. Krizhevsky, “Learning multiple layers of features from tiny images,” *University of Toronto*, 05 2012.
- [25] A. Krizhevsky, I. Sutskever, and G. E. Hinton, “Imagenet classification with deep convolutional neural networks,” in *Advances in Neural Information Processing Systems 25*, F. Pereira, C. J. C. Burges, L. Bottou, and K. Q. Weinberger, Eds. Curran Associates, Inc., 2012, pp. 1097–1105. [Online]. Available: <http://papers.nips.cc/paper/4824-imagenet-classification-with-deep-convolutional-neural-networks.pdf>
- [26] —, “Imagenet classification with deep convolutional neural networks,” in *Advances in neural information processing systems*, 2012, pp. 1097–1105.
- [27] A. Kurakin, I. Goodfellow, and S. Bengio, “Adversarial machine learning at scale,” *ArXiv*, vol. abs/1611.01236, 2017.
- [28] A. Kurakin, I. J. Goodfellow, and S. Bengio, “Adversarial examples in the physical world,” in *International Conference on Learning Representations (ICLR)*, 2017.
- [29] M. Lecuyer, V. Atlidakis, R. Geambasu, D. Hsu, and S. Jana, “Certified robustness to adversarial examples with differential privacy,” in *2019 IEEE Symposium on Security and Privacy (SP)*. IEEE, 2019, pp. 656–672.
- [30] C. R. Lefurgy, A. J. Drake, M. S. Floyd, M. S. Allen-Ware, B. Brock, J. A. Tierno, and J. B. Carter, “Active management of timing guardband to save energy in POWER7,” in *International Symposium on Microarchitecture (MICRO)*, December 2011, pp. 1–11.
- [31] J. Leng, Y. Zu, and V. J. Reddi, “Gpu voltage noise: Characterization and hierarchical smoothing of spatial and temporal voltage noise interference in gpu architectures,” in *2015 IEEE 21st International Symposium on High Performance Computer Architecture (HPCA)*, 2015, pp. 161–173.
- [32] F. Liao, M. Liang, Y. Dong, T. Pang, X. Hu, and J. Zhu, “Defense against adversarial attacks using high-level representation guided denoiser,” 2018.
- [33] G. Litjens, T. Kooi, B. E. Bejnordi, A. A. A. Setio, F. Ciompi, M. Ghafoorian, J. A. Van Der Laak, B. Van Ginneken, and C. I. Sánchez, “A survey on deep learning in medical image analysis,” *Medical image analysis*, vol. 42, pp. 60–88, 2017.
- [34] S. Ma, Y. Liu, G. Tao, W.-C. Lee, and X. Zhang, “Nic: Detecting adversarial samples with neural network invariant checking,” in *NDSS*, 2019.
- [35] X. Ma, B. Li, Y. Wang, S. M. Erfani, S. Wijewickrema, M. E. Houle, G. Schoenebeck, D. Song, and J. Bailey, “Characterizing adversarial subspaces using local intrinsic dimensionality,” *arXiv preprint arXiv:1801.02613*, 2018.
- [36] A. Madry, A. Makelov, L. Schmidt, D. Tsipras, and A. Vladu, “Towards deep learning models resistant to adversarial attacks,” in *International Conference on Learning Representations (ICLR)*, 2018.

- [37] A. Madry, A. Makelov, L. Schmidt, D. Tsipras, and A. Vladu, "Towards deep learning models resistant to adversarial attacks," 2019.
- [38] S. Majumdar, "Dense Net in Keras," <https://github.com/titu1994/DenseNet>.
- [39] J. H. Metzen, T. Genewein, V. Fischer, and B. Bischoff, "On detecting adversarial perturbations," 2017.
- [40] M. Mohammadi, A. Al-Fuqaha, S. Sorour, and M. Guizani, "Deep learning for IoT big data and streaming analytics: A survey," *IEEE Communications Surveys & Tutorials*, vol. 20, no. 4, pp. 2923–2960, 2018.
- [41] S.-M. Moosavi-Dezfooli, A. Fawzi, O. Fawzi, and P. Frossard, "Universal adversarial perturbations," in *2017 IEEE Conference on Computer Vision and Pattern Recognition (CVPR)*, 2017, pp. 86–94.
- [42] S.-M. Moosavi-Dezfooli, A. Fawzi, and P. Frossard, "Deepfool: A simple and accurate method to fool deep neural networks," in *IEEE Conference on Computer Vision and Pattern Recognition (CVPR)*, 2016.
- [43] K. Murdock, D. Oswald, F. D. Garcia, J. Van Bulck, D. Gruss, and F. Piessens, "Plundervolt: Software-based fault injection attacks against intel sgx," in *2020 IEEE Symposium on Security and Privacy (SP)*, 2020, pp. 1466–1482.
- [44] G. Papadimitriou, M. Kaliorakis, A. Chatzidimitriou, D. Gizopoulos, P. Lawthers, and S. Das, "Harnessing voltage margins for energy efficiency in multicore cpus," in *2017 50th Annual IEEE/ACM International Symposium on Microarchitecture (MICRO)*, 2017, pp. 503–516.
- [45] N. Papernot, P. McDaniel, A. Sinha, and M. Wellman, "Towards the science of security and privacy in machine learning," 2016.
- [46] N. Papernot, P. McDaniel, X. Wu, S. Jha, and A. Swami, "Distillation as a defense to adversarial perturbations against deep neural networks," in *2016 IEEE Symposium on Security and Privacy (SP)*, 2016, pp. 582–597.
- [47] N. Papernot, P. D. McDaniel, S. Jha, M. Fredrikson, Z. B. Celik, and A. Swami, "The limitations of deep learning in adversarial settings," in *IEEE European Symposium Security and Privacy*, 2016.
- [48] M. Pautov, G. Melnikov, E. Kaziakhmedov, K. Kireev, and A. Petiushko, "On adversarial patches: real-world attack on arcface-100 face recognition system," in *2019 International Multi-Conference on Engineering, Computer and Information Sciences (SIBIRCON)*. IEEE, 2019, pp. 0391–0396.
- [49] R. S. Raju and M. Lipasti, "Blurnet: Defense by filtering the feature maps," in *2020 50th Annual IEEE/IFIP International Conference on Dependable Systems and Networks Workshops (DSN-W)*. IEEE, 2020, pp. 38–46.
- [50] O. Russakovsky, J. Deng, H. Su, J. Krause, S. Satheesh, S. Ma, Z. Huang, A. Karpathy, A. Khosla, M. Bernstein, A. C. Berg, and L. Fei-Fei, "ImageNet Large Scale Visual Recognition Challenge," *International Journal of Computer Vision (IJCV)*, vol. 115, no. 3, pp. 211–252, 2015.
- [51] B. Salami, E. B. Onural, I. E. Yuksel, F. Koc, O. Ergin, A. C. Kestelman, O. S. Unsal, H. Sarbazi-Azad, and O. Mutlu, "An experimental study of reduced-voltage operation in modern fpgas for neural network acceleration," 2020.
- [52] B. Salami, O. S. Unsal, and A. Cristal Kestelman, "Comprehensive evaluation of supply voltage underscaling in fpga on-chip memories," in *2018 51st Annual IEEE/ACM International Symposium on Microarchitecture (MICRO)*, 2018, pp. 724–736.
- [53] Y. Sharma and P.-Y. Chen, "Attacking the madry defense model with L_1 -based adversarial examples," *arXiv preprint arXiv:1710.10733*, 2017.
- [54] —, "Bypassing feature squeezing by increasing adversary strength," *arXiv preprint arXiv:1803.09868*, 2018.
- [55] K. Simonyan and A. Zisserman, "Very deep convolutional networks for large-scale image recognition," 2014.
- [56] —, "Very deep convolutional networks for large-scale image recognition," 2015.
- [57] Y. Song, T. Kim, S. Nowozin, S. Ermon, and N. Kushman, "Pixeldefend: Leveraging generative models to understand and defend against adversarial examples," 2018.
- [58] C. Szegedy, W. Zaremba, I. Sutskever, J. Bruna, D. Erhan, I. Goodfellow, and R. Fergus, "Intriguing properties of neural networks," in *International Conference on Learning Representations 2014*, 2014.
- [59] X. Wang, R. Hou, B. Zhao, F. Yuan, J. Zhang, D. Meng, and X. Qian, "Dnnguard: An elastic heterogeneous dnn accelerator architecture against adversarial attacks," in *Proceedings of the Twenty-Fifth International Conference on Architectural Support for Programming Languages and Operating Systems*, ser. ASPLOS '20. New York, NY, USA: Association for Computing Machinery, 2020, p. 19–34. [Online]. Available: <https://doi.org/10.1145/3373376.3378532>
- [60] D. Warde-Farley, "1 adversarial perturbations of deep neural networks," 2016.
- [61] Xilinx, "CHaiDNN," <https://github.com/Xilinx/CHaiDNN>.
- [62] W. Xu, D. Evans, and Y. Qi, "Feature squeezing: Detecting adversarial examples in deep neural networks," in *Proceedings 2018 Network and Distributed System Security Symposium*, 2018.